DRAFT VERSION JANUARY 3, 2014
Preprint typeset using LaTeX style emulateapj v. 14/09/00

THE EVOLUTION OF THE TULLY–FISHER RELATION OF SPIRAL GALAXIES[1]

B. L. ZIEGLER[2], A. BÖHM, K. J. FRICKE, K. JÄGER, H. NICKLAS
Universitätssternwarte Göttingen, Geismarlandstr. 11, 37083 Göttingen, Germany
R. BENDER, N. DRORY, A. GABASCH, R. P. SAGLIA[3], S. SEITZ
Universitätssternwarte München, Scheinerstr. 1, 81679 München, Germany
AND
J. HEIDT, D. MEHLERT, C. MÖLLENHOFF, S. NOLL, E. SUTORIUS[4]
Landessternwarte Heidelberg, Königstuhl, 69117 Heidelberg, Germany
Draft version January 3, 2014

ABSTRACT

We present the *B*-band Tully–Fisher relation (TFR) of 60 late–type galaxies with redshifts $0.1-1$. The galaxies were selected from the FORS Deep Field with a limiting magnitude of $R = 23$. Spatially resolved rotation curves were derived from spectra obtained with FORS2 at the VLT. High-mass galaxies with $v_{\rm max} \gtrsim 150$ km/s show little evolution, whereas the least massive systems in our sample are brighter by $\sim 1-2$ mag compared to their local counterparts. For the entire distant sample, the TFR slope is flatter than for local field galaxies (-5.77 ± 0.45 versus -7.92 ± 0.18). Thus, we find evidence for evolution of the slope of the TFR with redshift on the 3σ level. This is still true when we subdivide the sample into three redshift bins. We speculate that the flatter tilt of our sample is caused by the evolution of luminosities and an additional population of blue galaxies at $z \gtrsim 0.2$. The mass dependence of the TFR evolution also leads to variations for different galaxy types in magnitude-limited samples, suggesting that selection effects can account for the discrepant results of previous TFR studies on the luminosity evolution of late–type galaxies.

Subject headings: galaxies: evolution — galaxies: kinematics and dynamics — galaxies: spiral

1. INTRODUCTION

Tully and Fisher (1977) found a remarkable correlation between the stellar content and the kinematics of disk galaxies linking tightly the luminosity to the maximum rotational velocity of late–type galaxies. This "Tully–Fisher Relation" (TFR) can therefore be exploited to study both the dynamical evolution and the star formation history of disk galaxies. Observed local TFR samples (e.g. Mathewson and Ford 1996) with their very small scatter already served as important constraints for galaxy evolution models (e.g. Eisenstein and Loeb 1996). But the redshift evolution of the TFR is an even more powerful tool to investigate galaxy evolution and cosmological structure formation.

On the observational side, recent studies of spiral galaxy kinematics at intermediate redshift produced rather discrepant results mainly due to different sample selection methods. While Vogt et al. (1996) find only a modest increase in luminosity of $\Delta M_B \approx 0.5$ at $\langle z \rangle \approx 0.5$, the results of Rix et al. (1997) and Simard and Pritchet (1998) imply a strong brightening of roughly 2 mag in absolute *B*-band luminosity.

Theoretical simulations have to consider the temporal growth of galaxies in size and mass as well as the evolution of the star formation rates. Mao et al. (1998), for example, combine the dynamical evolution as traced by Cold Dark Matter (CDM) hierarchical-merging models with a simple scaling relation between mass and luminosity. Steinmetz and Navarro (1999), in addition, introduce star formation phenomena via semianalytical recipes. These kind of studies predict zeropoint offsets in luminosity for distant TFR samples depending both on observed wavelength and cosmology.

2. SAMPLE AND OBSERVATIONS

Our galaxy sample is based on the FORS Deep Field (FDF), a deep multi-color study (*UBgRIzJK*) of an $\approx 6' \times 6'$ field with limiting blue and visual magnitudes comparable to the HST Deep Fields (Appenzeller et al. 2000; Heidt et al. 2001). Photometric redshifts and spectrophotometric galaxy types were determined for an *I*-band selected catalogue of ≈ 3800 objects (Bender et al. 2001). From this list, late-type galaxies were drawn primarily on the basis of their brightness with a limiting magnitude of $R < 23^m$ (as determined by the SExtractor package, Bertin and Arnouts 1996). Additional criteria have been that the inclination was $i > 40^\circ$ and $z_{\rm phot} < 1.2$ so that any [O II]3727 emission-line doublet would fall onto our observed wavelength range. The final sample comprised 79 spirals of all Hubble types (Sa – Irr) with $0.1 < z < 1.0$ peaking at $z = 0.35$ and 0.75 (see Fig. 1). Their absolute *B* magnitudes cover the range $-22.4 \leq M_B \leq -15.8$, the scale lengths range from 0.6 kpc to 4.8 kpc ($H_0 = 75\,{\rm km\,s^{-1}Mpc^{-1}}$ and $q_0 = 0$ assumed throughout the paper).

[1] Based on observations collected at the European Southern Observatory, Cerro Paranal, Chile (ESO Nos. 65.0-0049 & 66.A-0547).

[2] bziegler@uni–sw.gwdg.de

[3] Present address: Research School of Astronomy and Astrophysics, The Australian National University, Cotter Road, Weston Creek, ACT 2611, Australia

[4] Present address: Royal Observatory Edinburgh, Blackford Hill, Edinburgh EH9 3HJ, United Kingdom

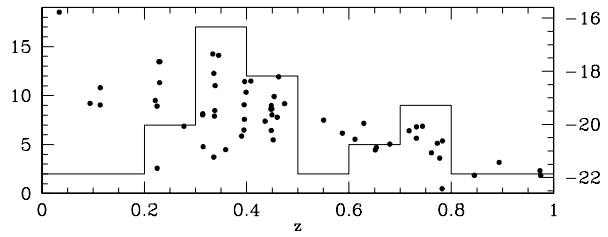

FIG. 1.— Redshift histogram of the FDF sample. Overplotted is the M_B distribution.

Spectroscopy was carried out with the Focal Reducer and Spectrograph 2 (FORS2) mounted onto the Very Large Telescope (VLT) Unit 2. Using the grism 600R with the order separation filter GG435, the typical wavelength range for the case of a chip-centered slit was $\lambda\lambda = 5250 - 7450$ Å. With a slit width of $1''$ the dispersion was 1.08 Å/pixel and the resolution $R \approx 1230$. Observations were done in MOS (Multi Object Spectroscopy) mode, in which FORS2 provides 19 slitlets of $\approx 22''$ length in a vertical array. Targets for the different setups were selected in a way to minimize the misalignment between slit direction and position angle of the galaxy. The maximal deviation was 15°. The exposures for each setup were split into 3×3000 s, the mean DIMM seeing was $0.66''$ (FWHM) for a spatial scale of $0.2''$/pixel. A detailed description of the reduction process will be given in Böhm et al. (2002).

3. DETERMINATION OF $v_{\rm max}$ AND M_b

To derive the rotation velocities of the galaxies as a function of radius, Gaussian profiles were fitted to the visible emission line(s). For the objects with high redshift ($0.4 \lesssim z \lesssim 1.0$), the [O II]3727 doublet was used, while for objects with $0.1 \lesssim z \lesssim 0.5$, the [O III]5007 and/or H_β lines were measured. To increase the S/N, a boxcar filter of $0.6''$ was applied, i.e. three neighbouring rows of the spectra were averaged before each Gaussian fit.

In contrast to studies of local spirals, these "straightforward" measurements of $v_{\rm rot}$(r) cannot be used to directly derive the maximum rotation velocity $v_{\rm max}$ (Simard and Pritchet 1999). Because the size of the visible disks of spirals at $z \approx 0.5$ (with typical apparent scale lengths of $r_d \approx 0.5''$) is comparable to the slit width of $1''$, the spectroscopy is an "integration" over the galaxies' intrinsic velocity fields.

To tackle this problem, a synthetic rotation curve (RC) was generated for each galaxy, assuming a linearly rising rotation velocity in the innermost galaxy regions and a constant rotation $v_{\rm max}$ at large radii (e.g. Courteau 1997). The radius at which this intrinsic RC flattens was computed from the scale length r_d measured in the *I*-band, taking into account that its value depends on the rest frame wavelength, because the scale length of the young star population is larger than that of the older population (Ryder and Dopita 1994). This intrinsic one-dimensional RC was then used to generate the 2D velocity field taking into account inclination and position angle. The structural parameters were derived from two-dimensional luminosity profile fits based on a coadded I-band image with an FWHM of $0.5''$. These fits considered the possible dependence of the Point Spread Function on CCD position. If a bulge was detectable, the fits included two components. To test our procedure, we performed a "VLT simulation" based on the drizzled HDF images by rebinning them to $0.2''$/pixel and convolving them to $0.5''$ FWHM. The disc inclinations we measured in these frames were then compared with the values given by Marleau and Simard (1998) based on the original images. For objects with B/T<0.4, the differences were limited to a few degrees. Estimated errors on the inclinations range from 7° for $i \approx 40°$ to 3° for $i \approx 80°$, in some cases they may be as high as up to 12°. In the next step, the inclined velocity field was folded with the luminosity profile and convolved to account for the seeing during spectroscopy. A simulated RC was extracted from the 2D velocity field by integrating over the slit aperture. At last, we variied $v_{\rm max}$, the only remaining free parameter in these simulations, until the best reproduction of the observed RC was achieved. In that manner we were able to quantify the maximum rotation velocity of 60 spirals in our sample, with estimated errors between 10 and 40 km/s, depending on galaxy size and RC quality. The remaining 19 objects showed either a solid–body rotation, highly disturbed RCs or no rotation at all. Examples of RCs are given in Fig. 2.

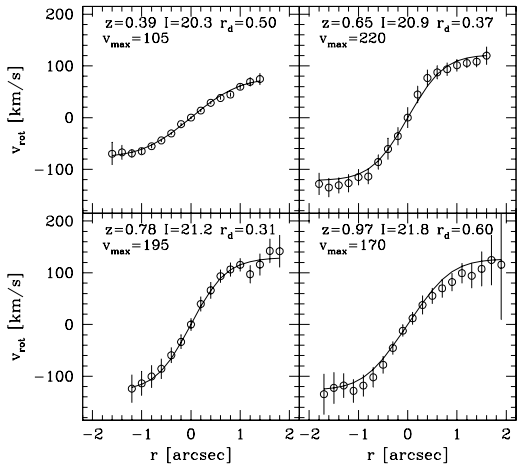

FIG. 2.— Examples of observed rotation curves with their 1D–fit. Respective values of redshift, $I_{\rm obs}$ magnitude, disk scale length (in arcsec) and $v_{\rm max}$ (as derived with the 2D–model of the velocity field) are given. Errorbars denote the errors of the Gaussian fits to the line positions.

The *B*-band luminosities of the FDF galaxies were determined in the following way: we took SExtractor's MAG_ISO values as the total magnitudes in the *BgRI* FORS2 filters, which were then transformed onto the Johnson–Cousins photometric system. One origin of uncertainty in the derivation of the rest–frame *B*-band luminosity is the *k*-correction (see e.g. Ziegler et al. 1999). For early-type spirals at $z \approx 1.0$, transformation from comoving to rest–frame *B*-band magnitude amounts to $\gtrsim 2$ mag. To keep the *k*-corrections small, we therefore used that filter which best matches the rest–frame *B*. Depending on the galaxies redshift, this was either the *B*-, *g*-, *R*- or *I*-band, leading to a typical correction of 0.5 mag. For the calculation of the respective *k*-corrections, we used template spectra created by the chemically consistent evolutionary synthesis models of Möller et al. (2001). Observed galaxy colors of different Hubble types (e.g. Frei and Gunn (1994)) are reproduced with these spectra to within 0.15 mag over the whole covered redshift range. Corrections for inclination-dependent intrinsic absorption due to dust were applied following Tully and Fouque (1985).

4. THE TULLY–FISHER RELATION AT $z \approx 0.5$

For the comparison to local data, we chose the large sample of 1196 field Sbc and Sc galaxies of Haynes et al. (1999). To be able to better compare our results with previous studies, we construct the *B*-band TFR in this letter (for the *I*-band and NIR TFR see Böhm et al. 2002). Therefore, the observed *I* magnitudes given by Haynes et al. were transformed to *B* using the type-dependent $(B-I)$ colors of Frei and Gunn (1994) and corrected for intrinsic absorption the same way as our sample. This transformation was tested on our sample (for which we both have *B* and *I* magnitudes), showing that on average the accuracy is within 0.1 mag independent of galaxy type. The resulting absolute magnitudes cover $-22.5 \leq M_B \leq -15.1$. For use in the TFR, we further corrected the derived M_B magnitudes for morphological and incompleteness bias following Giovanelli et al. (1997). The authors pointed out that an incompleteness bias arises from the differences between the luminosity function of a magnitude limited sample and the Schechter luminosity function. At low rotation velocities (low absolute magnitudes), galaxies falling below the detection limit do not contribute to the observed TFR, resulting in an underestimated slope. Simulating this, a synthetic, unbiased TFR is transformed into the observed relation using the measured values of $v_{\rm max}$, the observed scatter (as a function of $v_{\rm max}$) and the completeness limit. The effect can then be counter-balanced by decreasing the observed luminosities accordingly.

The magnitudes of the distant galaxies were de-biased with the same procedure adopting the parameterization of the scatter given by Giovanelli et al. but taking into account that the scatter in the FDF sample is on the mean 1.5 times larger. To account for the variation in the luminosity function with redshift, we subdivided our full FDF sample into three *z* bins, for which we constructed the observed luminosity functions separately. At the faint end of our sample, the correction for incompleteness amounts to maximal +1.4 mag. The morphological bias, as a similar effect, originates in the different luminosity functions for different morphological classes and leads to a slightly increased luminosity for early types ($\sim -0.3 ... -0.1$ mag). If not accounted for, the combination of these two biases leads to an underestimate of both slope and scatter of the TFR. We subdivided the 60 galaxies into 3 classes corresponding to Sa/Sb, Sc and Sd/Irr. This was done on the basis of spectrophotometric types from our photometric redshift catalog and by comparing our spectra to the catalog of template spectra of Kennicutt (1992). There are 10 Sa/b, 32 Sc and 18 Sd/Irr galaxies in our sample.

We present the distant *B*-band TFR in Fig. 3 in comparison to the local TFR. The FDF spirals follow a flatter relation than their local counterparts. While the most massive galaxies are indistinguishable on average from the local sample, the less massive galaxies show large deviations from the local fit. For the full FDF sample we find a slope of -5.77 ± 0.45 by repeating bisector fits (e.g. Ziegler et al. 2001) to the data centered on the median value of the $\log v_{\rm max}$-distribution ($\langle \log v_{\rm max} \rangle$ = 2.08) 100 times using a bootstrap method. For the local sample ($\langle \log v_{\rm max} \rangle$ = 2.182) the same method yields a slope of -7.92 ± 0.18. The last value is consistent with slopes derived for other local field samples. We derive, for example, a slope of −7.40 for the BBFN/RC3 sample (not de-biased; Burstein et al. 1997), and −7.50 for the Pierce and Tully (1992) sample. Sakai et al. (2000) find a slope of -8.07 ± 0.72 in the *B*-band using HST-based calibrators. Thus, the slopes of the local samples and the FDF sample differ on the 3σ level. This is confirmed by a 2D Kolmogorov–Smirnov test, which limits the probability that our sample originates from the same distribution as the Haynes et al. sample to 0.001. We also performed a simple Monte–Carlo simulation extracting randomly 60 galaxies from the local sample. Neither of 200 iterations resulted in a TFR slope as flat as for the FDF galaxies. If we subdivide our sample according to galaxy type (Sa/b, Sc and Sd/Irr) or redshift, the resulting slopes and zero-points are compatible with each other within their 1σ errors (see Table 1).

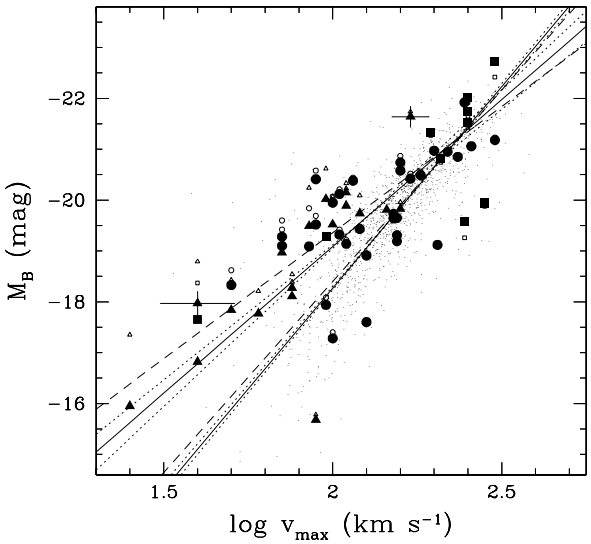

FIG. 3.— The *B*-band Tully–Fisher relation of 60 field spiral and irregular galaxies at intermediate redshifts. Big symbols denote our spectrophotometric classification: squares Sa/Sb, circles Sc, triangles Sd/Irr. Open symbols correspond to "observed" data, filled symbols to de-biased data. Solid (dotted) lines represent the best ($\pm 1\sigma$) fits of the 100 bootstrap bisector fits to the de-biased sample. The dashed lines are the fits to the "observed" data. The steeper lines show similar fits to the large sample of 1200 local field spirals (dots) from Haynes et al. (1999). There is a clear change of slope (on the 3σ level) between the local and distant TFR. Two typical errorbars are given.

TABLE 1
TFR SLOPES WITH 1σ ERRORS

sample	*N*	M_B vs. $\log v$	$\log v$ vs. M_B
distant sample:			
FDF (not de-biased)	60	-4.99 ± 0.48	-0.202 ± 0.016
FDF	60	-5.77 ± 0.45	-0.175 ± 0.014
FDF $z < 0.3$	11	-5.46 ± 0.68	-0.195 ± 0.054
FDF $0.3 \leq z < 0.5$	29	-4.62 ± 0.48	-0.220 ± 0.026
FDF $z \geq 0.5$	20	-5.59 ± 0.61	-0.174 ± 0.014
local samples:			
Haynes et al. (not de-biased)	1296	-7.52 ± 0.18	-0.133 ± 0.003
Haynes et al. (1999)	1296	-7.92 ± 0.18	-0.126 ± 0.003
BBFN (not de-biased)	467	-7.40 ± 0.21	-0.135 ± 0.004
Sakai et al. (2000)	21	-8.07 ± 0.72	

Can the observed change of slope be caused by systematic errors? Any overestimate of *i* would both lead to an underestimate of $v_{\rm max}$ and too large a luminosity after correcting for intrinsic absorption. But to introduce a significant effect on the slope, the errors on *i* would have to be large: assuming, e.g., an inclination of 60° instead of 40° for an object, the shift in the TFR with a slope of −6 would amount to −0.93 mag. Such measurement errors are unlikely, as our inclinations do not show any dependence on rotation velocity nor apparent scale length

nor type. For that reason, we are also confident that morphologically irregular objects in our sample are unlikely to have introduced a significant bias in the inclinations.

5. DISCUSSION

Our intermediate-z TFR indicates a change in the slope with look–back time. Most previous studies of the kinematics of spirals in this regime were restricted to small data sets ($N \lesssim 20$) and had to assume a constant slope. In the ongoing study of Vogt (2000) of ~ 100 distant disk galaxies, it was also assumed that the slope of the local TFR of Pierce and Tully (1992) holds valid at all redshifts.

CDM-based simulations predict a slight brightening of the B-band TFR up to $z = 1$ (e.g. Steinmetz and Navarro 1999). In this model, the decrease in mass is more than balanced by an increase in luminosity due to younger stellar populations. Any mass-dependent evolution of the star formation rate or other TF parameters that would cause an evolving TFR slope are yet not implemented in these models.

A change in the TFR slope as we observed makes it impossible to give a single number for the luminosity evolution of distant galaxies since it depends on the galaxy mass. The FDF galaxies with $v_{\rm max} \gtrsim 150$ km/s fall into the same magnitude region as those of the local sample and show no significant luminosity evolution, whereas the less massive distant galaxies are brighter by $\sim 1-2$ mag.

A mass dependence of the TFR evolution also introduces a dependence on galaxy type since the various sub-classes of disk galaxies have different distributions in mass ($\log v_{\rm max}$) for a magnitude–limited sample. Thus, a natural explanation of the discrepant results in luminosity evolution of previous observational studies is suggested. For example, studies based on samples with galaxies selected to be blue (like Rix et al. 1997) or showing strong emission lines (like Simard and Pritchet 1998) are biased towards later types of spirals (de Vaucouleurs 1961; Kennicutt and Kent 1983) resulting in a large luminosity increase. On the other hand, studies using mainly galaxies with large disks (like Vogt et al. 1996) may contain a larger fraction of early and luminous spirals leading to a more modest luminosity evolution.

At last, we speculate on the possible origin of the flatter tilt in all three redshift bins ($z < 0.3, 0.3 \le z < 0.5, z \ge 0.5$). A plausible scenario would be that we not only trace a pure luminosity evolution but also observe a population of blue dwarf galaxies with $M_B > -20$ underrepresented in the local Universe. This would be consistent with blue number counts that suggest a higher number density of bursting dwarfs at $z \lesssim 0.5$ (e.g. Ellis 1997). These objects may have too low a rotation for their luminosity as observed by Rix et al. (1997). On the other hand, the star formation rates of all FDF galaxies ($0.2-18\,M_\odot/{\rm yr}$) fall well below the local regime of starburst galaxies (Kennicutt 1998). If we exclude the low-mass objects with $v_{\rm max} < 80$ km/s and $M_B > -18$ ($N = 16$) from the local and distant sample, we derive slopes of -7.29 ± 0.15 and -5.08 ± 0.50, respectively, confirming the change of tilt with 3σ confidence.

6. SUMMARY

We have presented the B-band Tully–Fisher relation of 60 disk galaxies at intermediate redshifts. The galaxies comprise a magnitude-limited sample within the FORS Deep Field. We observe a significant (3σ) change of slope in comparison to the local sample. The larger FDF spirals ($v_{\rm max} \gtrsim 150$ km/s) fall into a region of the $\log v_{\rm max}$ – luminosity diagram consistent with modest or no luminosity evolution. On the contrary, the smaller distant galaxies are offset from the local TFR by order $\sim 1-2$ mag.

We acknowledge the continuous support of our project by the PI of the FDF consortium, Prof. I. Appenzeller. We also thank ESO and the Paranal staff for efficient support of the observations. Our work was funded by the Volkswagen Foundation (I/76 520), the Deutsche Forschungsgemeinschaft (SFB375, SFB439) and the German Federal Ministry for Education and Science (ID–Nos. 05 AV9MGA7, 05 AV9WM1/2, 05 AV9VOA).

REFERENCES

Appenzeller, I., et al. 2000, The Messenger, 100, 44.
Bender, R., et al. 2001, ESO/ECF/STScI Workshop on Deep Fields, 327.
Bertin, E. and Arnouts, S. 1996, A&AS, 117, 393.
Böhm, A., et al. 2002, in preparation.
Burstein, D., Bender, R., Faber, S. and Nolthenius, R. 1997, AJ, 114, 1365.
Courteau, S. 1997, AJ, 114, 2402.
de Vaucouleurs, G. 1961, ApJS, 5, 233.
Eisenstein, D. J. and Loeb, A. 1996, ApJ, 459, 432.
Ellis, R. S. 1997, ARA&A, 35, 389.
Frei, Z. and Gunn, J. E. 1994, AJ, 108, 1476.
Giovanelli, R., Haynes, M. P., Herter, T., Vogt, N. P., da Costa, L. N., Freudling, W., Salzer, J. J., and Wegner, G. 1997, AJ, 113, 53.
Haynes, M. P., Giovanelli, R., Chamaraux, P., da Costa, L. N., Freudling, W., Salzer, J. J., and Wegner, G. 1999, AJ, 117, 2039.
Heidt, J., et al. 2001, Reviews in Modern Astronomy No. 14, 209.
Kennicutt, R. C. and Kent, S. M. 1983, AJ, 88, 1094.
Kennicutt, R. C. 1992, ApJ, 388, 310.
Kennicutt, R. C. 1998, ARA&A, 36, 189.
Marleau, F. R. and Simard, L. 1998, ApJ, 507, 585.
Mao, S., Mo, H. J. and White, S. D. M. 1998, MNRAS, 295, 319.
Mathewson, D. S. and Ford, V. L. 1996, ApJS, 107, 97.
Möller, C. S., Fritze–v. Alvensleben, U. and Calzetti, D. 2001, MNRAS, submitted.
Pierce, M. J. and Tully, R. B. 1992, ApJ, 387, 47.
Rix, H.-W., Guhathakurta, P., Colless, M. and Ing, K. 1997, MNRAS, 285, 779.
Ryder, S. D. and Dopita, M. A. 1994, ApJ, 430, 142.
Sakai, S. et al. 2000, ApJ, 529, 698.
Simard, L. and Pritchet, C. J. 1998, ApJ, 505, 96.
Simard, L. and Pritchet, C. J. 1999, PASP, 111, 453.
Steinmetz, M. and Navarro, J. F. 1999, ApJ, 513, 555.
Tully, R. B. and Fisher, J. R. 1977, A&A, 54, 661.
Tully, R. B. and Fouque, P. 1985, ApJS, 58, 67.
Vogt, N. P. 2000, in ASP Conf. Ser. 197: Dynamics of Galaxies: from the Early Universe to the Present, 435.
Vogt, N. P., Forbes, D. A., Phillips, A. C., Gronwall, C., Faber, S. M., Illingworth, G. D. and Koo, D. C. 1996, ApJ, 465, L15.
Ziegler, B. L., Saglia, R. P., Bender, R., Belloni, P., Greggio, L. and Seitz, S. 1999, A&A, 346, 13.
Ziegler, B. L., Bower, R. G., Smail, I. R., Davies, R. L. and Lee, D. 2001, MNRAS, 325, 1571.